Decentralized Stability Criteria for Grid-Forming Control in Inverter-Based Power Systems

Zudika Siahaan, Enrique Mallada, and Sijia Geng

Abstract—This paper presents a decentralized stability analysis of power systems comprising grid-forming (GFM) inverters. We leverage a decentralized stability framework capable of ensuring the stability of the entire interconnection through individual assessments at each bus. The key novelty lies in incorporating voltage dynamics and their coupling with reactive power, in addition to the angle dynamics and their coupling with active power. We perform loop transformation to address the challenge posed by the non-Laplacian nature of the network Jacobian matrix in this case. This methodology is applied to characterize conditions on the droop gains of GFM controllers that can preserve system-wide stability. Our proposed stability criteria exhibit scalability and robustness, and can be extended to accommodate delays, variations in network conditions, and plugand-play of new components in the network.

Index Terms—Stability, decentralized criteria, grid-forming inverters, power systems, robustness.

I. INTRODUCTION

Increasing shares of renewable generation are being deployed worldwide as a major effort to transition towards more sustainable power systems [1]. The ongoing transition leads to significant challenges for maintaining system stability due to substituting synchronous machines (and their well-known dynamics) with inverter-based resources (IBRs) whose dynamics and interaction with the rest of the system are yet to be fully understood [2]. For example, the West Murray Zone is a region in Australia that has significant penetration of renewable IBRs and low system strength. The Australian Energy Market Operator (AEMO) has observed subsynchronous oscillations (SSO) of 16 to 19 Hz in that region on various occasions from August 2020 through December 2021 [3].

Future power systems will host a mix of heterogeneous resources including synchronous machines and numerous distributed IBRs that interact with each other through the network. It is imperative to develop rigorous and efficient methods that can ensure system stability under this circumstance. However, there are many challenges. First, system dynamics will become much more complex. Conventional stability analysis approaches such as eigenvalue analysis [4] and transient stability analysis [5] will face significant computational challenges, especially when detailed inverter models are considered [6]-[9]. Moreover, the unpredictable nature of renewable generation introduces significant variability in operating points, further contributing to the challenge. Most importantly, unlike the case for synchronous machines whose dynamics are governed by physics, the IBR dynamics, as seen from the system level, are dictated by the implemented controllers. However, due to the proprietary designs of IBRs,

Zudika Siahaan, Enrique Mallada, and Sijia Geng are with the Department of Electrical and Computer Engineering, Johns Hopkins University, Baltimore, MD 21218, USA. Corresponding Author: Sijia Geng (email: sgeng@jhu.edu).

there is a lack of transparency in control implementations, which leaves the system more obscure for grid operators [10] and makes model-based methods such as the well-known energy function-based method [11] challenging be to applied.

To overcome these challenges, in this paper, we extend the decentralized stability framework introduced in [12] to establish decentralized stability criteria for IBR-based power systems. These criteria, derived from local device dynamics, ensure system-wide stability with the need for certification only at the individual component level. The key novelty in our development lies in incorporating voltage dynamics (in addition to the angle dynamics) and the coupling between reactive power and voltage magnitude (in addition to the coupling between active power and angle) to model IBR dynamics. However, integrating voltage dynamics prevents the method from being trivially applicable to the power system model of interest. The primary bottleneck in this case is the non-Laplacian nature of the network Jacobian matrix, characterized by non-zero row sums. To address this challenge, we perform loop transformation to achieve an equivalent network feedback interconnection. Subsequently, we apply the decentralized stability analysis, combined with the Gershgorin's Circle Theorem, to characterize conditions on the droop gains of grid-forming (GFM) inverters that can preserve system-wide stability. We further illustrate and verify the efficacy of our decentralized stability criteria through numerical examples. Finally, it is worth mentioning that, the constructed stability condition inherently exhibits robustness to changes in operating points and network configurations, accommodating seamless integration or removal of devices.

II. PRELIMINARIES

A. Notation

Vector: We use $\text{vec}(\{x_i\}_{i\in\mathcal{V}}) = [x_1^T, x_2^T, \dots, x_p^T]^T$ to denote a stacked vector based on the ordering in the index set $\mathcal{V} = \{1, 2, \dots, p\}$.

Matrix: We define the identity matrix by I. We define $\operatorname{diag}(\{a_i\}_{i\in\mathcal{V}})$ to be a matrix that has terms a_i sitting on the diagonal in order and zero elsewhere. For two Hermitian matrices $A,B\in\mathbb{C}^{n\times n}$, we write $A\succeq B$ if A-B is positive semi-definite.

Graph: For a connected graph $\mathcal{G} = (\mathcal{V}, \mathcal{E})$, \mathcal{V} and \mathcal{E} denote the set of buses and edges, respectively. Let $\mathcal{N}_i \triangleq \{j \in \mathcal{V} : (i,j) \in \mathcal{E}\}$ be the set of buses who are adjacent to bus i.

Transfer function: We denote the space of transfer function of stable linear time-invariant systems by \mathscr{H}_{∞} , describing the Hardy space of functions that are analytic on the open right half-plane $\mathbb{C}_{>0}$ with bounded norm $\|g(s)\|_{\infty} := \sup_{s \in \mathbb{C}_{>0}} |g(s)|$. We denote the subset of \mathscr{H}_{∞} that is continuous on the extended imaginary axis by \mathscr{A}_{0} .

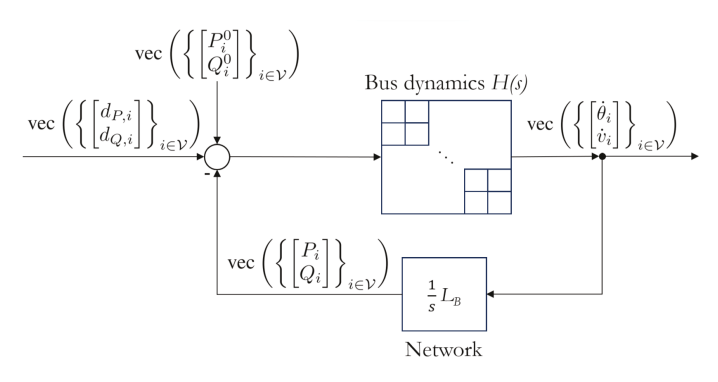


Figure 1. Block diagram of the power system model.

In this paper, we concentrate our analysis on IBR-based power systems¹. We consider a (connected) network-reduced power system consisting of buses indexed by $\mathcal{V} := \{1, \ldots, \}$ N}, where N denotes the number of IBRs in the network, with the block diagram structure given in Fig. 1. Without loss of generality, we assume that the first node provides an angle reference to the rest of the network. We denote each transmission line by the unordered pair $(i, k) \in \mathcal{E}$. We define the following:

$$\operatorname{vec}\left(\left\{\begin{bmatrix}P_i\\Q_i\end{bmatrix}\right\}_{i\in\mathcal{V}}\right) = [P_1,Q_1,\ldots,P_N,Q_N]^T.$$

We use similar definitions for $\text{vec}(\{[d_{P,i}, d_{Q,i}]^T\}_{i \in \mathcal{V}}\})$, $\text{vec}(\{[P_i^0, Q_i^0]^T\}_{i \in \mathcal{V}}\}), \text{ and } \text{vec}(\{[\dot{\theta}_i, \dot{V}_i]^T\}_{i \in \mathcal{V}}\}).$

The closed-loop system is modeled as the feedback interconnection of bus dynamics H(s) and the linearized network model $\frac{1}{s}L_B$. For the *i*-th bus, the exogenous signals $[P_i^0,\ Q_i^0]^T\in\mathbb{R}^{2 imes 1}$ and $[d_{P,i},\ d_{Q,i}]^T\in\mathbb{R}^{2 imes 1}$ respectively represent the power injection setpoint and power fluctuations around the setpoint that indicates, for example, variations in power drawn by local loads. The output signals $[\dot{\theta}_i,\dot{V}_i]^T \in \mathbb{R}^{2 \times 1}$ represent the bus frequency and voltage derivative, respectively. Through the network, the signals $[\theta_i^{V},\ _i]^T$ are mapped to the power demand $[P_i,Q_i]^T$. Furthermore, we make the following assumptions for the power system model. First, transmission lines are lossless. Second, at equilibrium, the angle difference across each transmission line is less than 90°. These assumptions are well-justified and generally hold for most transmission systems [13]. In addition, we use $V_{\max,0j}$ to represent the maximum per unit steady state voltage magnitude of bus j. We denote the maximum steady state voltage among all buses j neighboring bus i as $\max_{j \in \mathcal{N}_i} \{V_{0j}\}.$

We now discuss the model of the different components in the system in more detail.

1) Bus dynamics: In this paper, we work with droop-based GFM inverters. The dynamics are composed of the droopbased control laws described by [6], [14],

$$\begin{cases} \dot{\theta}_{i} = \omega_{i} \\ \omega_{i} = \omega_{i}^{0} + m_{i}^{p} f_{i}^{p}(s) ((P_{i}^{0} + d_{P,i}) - P_{i}), & \forall i \in \mathcal{V}, \\ V_{i} = V_{i}^{0} + m_{i}^{q} f_{i}^{q}(s) ((Q_{i}^{0} + d_{Q,i}) - Q_{i}), \end{cases}$$

where $m_i^p \in \mathbb{R}_{>0}$ and $m_i^q \in \mathbb{R}_{>0}$ are the droop gains; ω_i^0 and V_i^0 are the frequency and voltage setpoints; P_i^0 and Q_i^0 are the power setpoints; $f_i^p(s) = \frac{\beta_i^p}{\tau_i^p s + 1}$ and $f_i^q(s) = \frac{\beta_i^q}{\tau_i^q s + 1}$ represent the low-pass filters applied to the power measurements with DC gains $\beta_i^p \in \mathbb{R}_{>0}$ and $\beta^q \in \mathbb{R}_{>0}$, and time constants $\tau^q \in \mathbb{R}_{>0}$ and $\tau^p \in \mathbb{R}_{>0}$. Substituting in the expression of low-pass

filters, we

get
$$\omega_{i} = \omega_{i}^{0} + \begin{pmatrix} \frac{m_{i}^{p}\beta_{i}^{p}}{s+1} \end{pmatrix} ((P_{i}^{0} + d_{P,i}) - P_{i})$$
(2)
$$\dot{V}_{i} = \dot{V}_{i}^{0} + \begin{pmatrix} \frac{\tau_{i}\beta_{i}^{q}s}{t_{i}^{p}s+1} \end{pmatrix} ((Q_{i}^{0} + d_{Q,i}) - Q_{i})$$
(3)

$$\dot{V}_{i} = \dot{V}_{i}^{\Theta} \qquad \left(\frac{\tau_{i} \beta_{i}^{q} s}{\tau_{i}^{q} s + 1}\right) \left(\left(Q_{i}^{0} + d_{Q,i}\right) - Q_{i}\right) \tag{3}$$

which respectively give the following transfer functions of frequency and voltage dynamics:

$$h_i^{\theta}(s) = \frac{m_i^p \beta_i^p}{\tau_i^p s + 1},\tag{4}$$

$$h_i^V(s) = \frac{m_i^q \beta_i^q s}{m_{ij}^q s + 1}.$$
 (5)

The term $m_i^p \beta_i^p$ and $m_i^q \beta_i^q$ represent the effective droop gains. Furthermore, the matrix of bus dynamics H(s) is modeled as

$$H(s) = \left(\operatorname{diag}\left\{\operatorname{diag}(h_i^{\theta}(s), h_i^{V}(s))\right\}_{i \in \mathcal{V}}. (6)\right)$$

Remark 1. The chosen GFM inverter model (1) is relatively simplified because we intend to capture important system-level dynamics. For future studies involving more detailed inverter modeling, for example, incorporating lower-level control loops and integrating various other devices into a multi-machine multi-inverter system, we anticipate dynamic coupling between voltage magnitude V and angle θ in the bus dynamics. This coupling is expected to result in a multi-input-multi-output (MIMO) non-diagonal matrix H.

2) Network model: We consider linearized decoupled power flow equations. This is under the assumption of a lossless network with small angle differences in steady state, which results in very weak coupling between P-V, as well as $Q-\theta$. It is important to note that this assumption may not hold in scenarios such as a low voltage distribution system with a high R/X ratio or in a microgrid. The network model is given by,

$$\operatorname{vec}\left(\left\{\begin{bmatrix} P_i \\ Q_i \end{bmatrix}\right\}_{i \in \mathcal{V}}\right) = \frac{1}{s} L_B \operatorname{vec}\left(\left\{\begin{bmatrix} \dot{\theta}_i \\ \dot{V}_i \end{bmatrix}\right\}_{i \in \mathcal{V}}\right) \tag{7}$$

where

$$L_B = \begin{bmatrix} \tilde{P}_{\theta,11} & 0 & \dots & \tilde{P}_{\theta,1N} & 0 \\ 0 & \tilde{Q}_{v,11} & \dots & 0 & \tilde{Q}_{v,1N} \\ \vdots & \vdots & \ddots & \vdots & \vdots \\ \tilde{P}_{\theta,N1} & 0 & \dots & \tilde{P}_{\theta,NN} & 0 \\ 0 & \tilde{Q}_{v,N1} & \dots & 0 & \tilde{Q}_{v,NN} \end{bmatrix} \in \mathbb{R}^{2N \times 2N},$$

 $^{^1\}mathrm{Although}$ the results can be generalized to encompass a mix of synchronous machines and various types of IBRs, we restrict to the homogeneous IBR-based systems due to space limitation.

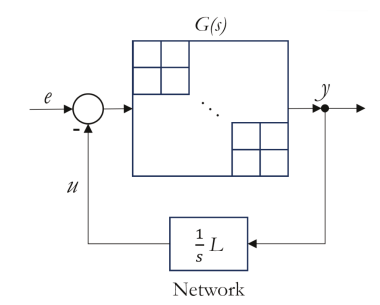


Figure 2. General feedback interconnection.

and

$$\tilde{P}_{\theta,ij} = \frac{\partial}{\partial \theta_j} \sum_{l \in \mathcal{N}_i} -V_i V_l B_{il} \sin(\theta_i - \theta_l) \Big|_{\substack{\theta = \theta_0 \\ V = V_0}} \\
= \begin{cases}
-\sum_{l \in \mathcal{N}_i} V_{0i} V_{0l} B_{il} \cos(\theta_{0i} - \theta_{0l}), & i = j, \\
V_{0i} V_{0j} B_{ij} \cos(\theta_{0i} - \theta_{0j}), & i \neq j,
\end{cases} \\
\tilde{Q}_{V,ij} = \frac{\partial}{\partial V_j} \left(V_i^2 B_{ii} + \sum_{l \in \mathcal{N}_i} V_i V_l B_{il} \cos(\theta_i - \theta_l) \right) \Big|_{\substack{\theta = \theta_0 \\ V = V_0}} \\
= \begin{cases}
2V_{0i} B_{ii} + \sum_{l \in \mathcal{N}_i} V_{0l} B_{il} \cos(\theta_{0i} - \theta_{0l}), & i = j, \\
V_{0i} B_{ij} \cos(\theta_{0i} - \theta_{0j}), & i \neq j.
\end{cases} \tag{8}$$

In these equations, $V_0 \in \mathbb{R}^N$ and $\theta_0 \in \mathbb{R}^N$ denote the voltage magnitudes and angles at the buses in steady state. The term $B_{ik} \leq 0 \ (\forall i \neq k)$ denotes the mutual susceptance of the transmission line connecting buses i and k, $B_{ik} = 0$ if there is no line, and $B_{ii} = -\sum_{k \in \mathcal{N}_i} B_{ik} \geq 0$ denotes the self susceptance of bus i.

III. MAIN RESULTS

In this section, we develop the main decentralized stability criteria for GFM IBR-based power systems. Note that this result can be extended to more general scenarios in multimachine multi-inverter systems. Due to the space limitation, we defer the discussion of such cases in future work.

We build on a decentralized stability result [12, Th. 1], which is replicated below in **Theorem 1**. The theorem is applicable to a general feedback interconnection as in Fig. 2 with single-input-single-output (SISO) bus dynamics (therefore diagonal matrix G(s)) and network model $\frac{1}{s}L$. The system equations are described by,

$$y_i(s) = g_i(s)(e_i(s) - u_i(s)),$$

$$\underline{1}$$

$$u(s) = {}_{S}Ly(s).$$
(9)

Theorem 1. [12, Th. 1] Let PR and ESPR denote the set of positive real and extended strictly positive real functions, respectively. If there exists a function $f(s) \in PR \cap \mathcal{A}_0$ where for all bus dynamics it holds that $g(s) \in \mathcal{G}_f$, where

$$\begin{split} \mathcal{G}_f &:= \{g(s) \in \mathscr{H}_\infty \colon \\ g(0) &\neq 0, \, f(s) \, \left(1 + \frac{g(s)}{s}\right) \in ESPR \}, \end{split}$$

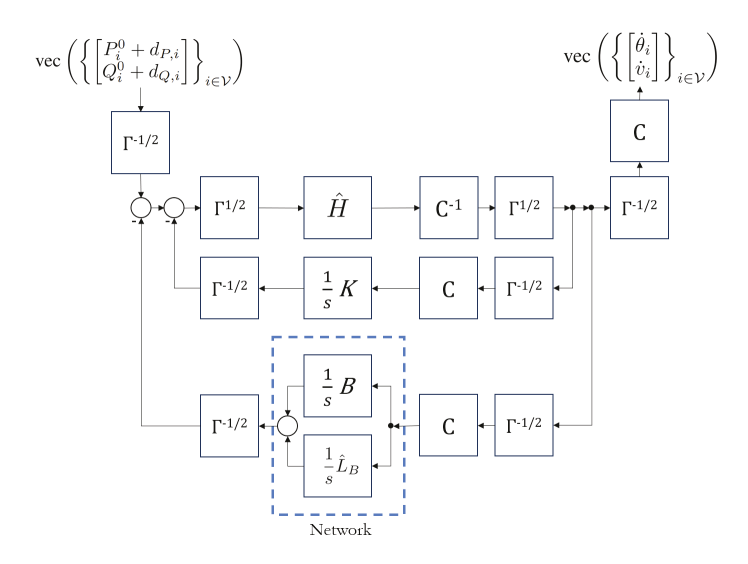


Figure 3. Equivalent system to Fig. 1 unto loop transformation.

then the feedback interconnection in (9) is stable for any network model $L \in \mathcal{L}$, where

$$\mathcal{L} := \{ L : L = L^T, 0 \prec L \prec I \}.$$

Remark 2. The key strengths of **Theorem 1** include its capability to handle cases when components are added or removed from the network, and when the operating point changes [12].

A. Application to IBR-Based Power Systems

We observe that the dynamics of voltage angle and magnitude in (6) are completely decoupled. Consequently, we can treat our model of interest as having separate SISO dynamics, allowing us to utilize the result from **Theorem 1** to formulate the decentralized stability criteria. The key challenge that prevents the application of **Theorem 1** to the power system configuration in Fig. 1 lies in that L_B is not necessarily in \mathcal{L} . In this section, we address this challenge by performing loop transformation. We define the following terms,

$$\begin{split} \hat{h}_{i}^{V}(s) &:= m_{i}^{q} \beta_{i}^{q} / \tau_{i}^{q}, \\ k_{i} &:= 1 / m_{i}^{q} \beta_{i}^{q}, \\ \gamma_{i}^{p} &:= 2 \sum_{j \in \mathcal{N}_{i}} V_{\max,0i} V_{\max,0j} B_{ij}, \\ \gamma_{i}^{q} &:= k_{i} V_{\max,0i} + 2 V_{\max,0i}^{2} B_{ii}, \\ \hat{H}(s) &:= \operatorname{diag}(\{\operatorname{diag}(h_{i}^{\theta}(s), \hat{h}_{i}^{V}(s))\}_{i \in \mathcal{V}}), \\ K &:= \operatorname{diag}(0, k_{1}, 0, k_{2}, \dots, 0, k_{N}), \\ \Gamma &:= \operatorname{diag}(\gamma_{1}^{p}, \gamma_{1}^{q}, \gamma_{2}^{p}, \gamma_{2}^{q}, \dots, \gamma_{N}^{p}, \gamma_{N}^{q}), \\ C &:= \operatorname{diag}(1, V_{01}, 1, V_{02}, \dots, 1, V_{0N}), \\ B &:= \operatorname{diag}(0, 2 V_{01} B_{11}, 0, 2 V_{02} B_{22}, \dots, 0, 2 V_{0N} B_{NN}), \\ \hat{L}_{B} &:= L_{B} - B. \end{split}$$

It can be shown that the block diagram in Fig. 1 can be transformed equivalently into Fig. 3, with the corresponding terms defined above. Upon combining the two feedback

branches in Fig. 3, we obtain that the corresponding G(s) and L in Fig. 2 are defined by

$$G(s) = \Gamma^{1/2}C^{-1}\hat{H}(s)\Gamma^{1/2},$$

$$L = \Gamma^{-1/2}((K+B) + \hat{L}_B)C\Gamma^{-1/2}.$$
(11)

Next, we show that, facilitated by the loop transformation, the resulting L in (11) can be made to satisfy $0 \le L \le I$.

Lemma 1. *If for all buses* $i \in V$ *it holds that*

$$\left(\max_{j \in \mathcal{N}_i} \{V_{0j}\} - V_{0i}\right) \beta_i^q \le \frac{1}{2m_i^q |B_{ii}|},\tag{12}$$

then L as given by (11) satisfies $0 \leq L \leq I$.

Proof. By definition in (11), L is symmetric. As a consequence of Gershgorin's Circle Theorem [15], the eigenvalues of matrix $L:=\{l_{ij}\}$ live in a ball centered at l_{ii} of radius $\sum_{j\in\mathcal{N}_i}l_{ij}$. Let $\pi:\{1,\ldots,N\}\longrightarrow\{1,\ldots,N\}$ be a bijection. Then every odd row i in L satisfies

$$\lambda_{\pi(i)}(L) \ge l_{ii} - \sum_{j \in \mathcal{N}_i} |l_{ij}|$$

$$= \frac{1}{\gamma_i^p} \sum_{j \in \mathcal{N}_i} |V_{0i} V_{0j} B_{ij} \cos(\theta_{0i} - \theta_{0j})|$$

$$- \sum_{j \in \mathcal{N}_i} \left| \frac{1}{\gamma_i^p} V_{0i} V_{0j} B_{ij} \cos(\theta_{0i} - \theta_{0j}) \right| = 0.$$
(13)

For every even row i, Gershgorin's Circle Theorem gives

$$\lambda_{\pi(i)}(L) \ge l_{ii} - \sum_{j \in \mathcal{N}_i} |l_{ij}| \ge \frac{1}{\gamma_i^q} k_i V_{0i} + \frac{2}{\gamma_i^q} V_{0i}^2 B_{ii}$$

$$+ \frac{1}{\gamma_i^q} \sum_{j \in \mathcal{N}_i} V_{0i} V_{0j} B_{ij} \cos (\theta_{0i} - \theta_{0j})$$

$$- \sum_{i \in \mathcal{N}_i} |\frac{1}{\gamma_i^q} V_{0i} V_{0j} B_{ij} \cos (\theta_{0i} - \theta_{0j})|.$$
(14)

Now, suppose the voltage magnitude at each bus j neighboring bus i satisfies (12). Then,

$$k_{i} \geq 2 \left(\max_{j \in \mathcal{N}_{i}} \{V_{0j}\} - V_{0i} \right) |B_{ii}|$$

$$\geq 2 \sum_{j \in \mathcal{N}_{i}} \max_{j \in \mathcal{N}_{i}} \{V_{0j}\} |B_{ij}| - 2V_{0i} |B_{ii}|.$$
(15)

Since $\frac{1}{\gamma_i}V_{0i} \ge 0$, (15) ensures $\lambda_{\pi(i)} \ge 0$ for all even i in (14). Therefore, L is positive semi-definite, or $L \succeq 0$, as a direct consequence of (13), (14), and (15).

Furthermore, we want to prove that it holds that $L \leq I$ with a similar reasoning. For every odd row i, Gershgorin's Circle Theorem gives $\lambda_{\pi(i)}(I-L)$ satisfies

$$\lambda_{\pi(i)}(I-L) \ge (1-l_{ii}) - \sum_{j \in \mathcal{N}_i} |l_{ij}|$$

$$= 1 - \frac{2}{\gamma_i^p} \sum_{j \in \mathcal{N}_i} |V_{0i}V_{0j}B_{ij}\cos(\theta_{0i} - \theta_{0j})|$$

$$\ge 0.$$
(16)

For every even row i, Gershgorin's Circle Theorem gives

$$\lambda_{\pi(i)}(I - L) \ge (1 - l_{ii}) - \sum_{j \in \mathcal{N}_i} |l_{ij}|$$

$$= 1 - \frac{1}{\gamma_i^q} \left(k_i V_{0i} + 2V_{0i}^2 B_{ii} \right)$$

$$> 0.$$
(17)

Thus, (16) and (17) imply $I-L\succeq 0$ or, equivalently, $I\succeq L$. Therefore, satisfying (12) implies $0\preceq L\preceq I$.

B. Decentralized Stability Criteria for IBR-Based Systems

Combining the results in **Theorem 1** and **Lemma 1**, we derive the final result on decentralized stability criteria for droop-controlled IBR-based power systems.

Theorem 2. Given the feedback interconnection in Fig. 1 consisting of droop-controlled IBRs whose dynamics are given in (1), with the droop constants $m^p \in \mathbb{R}^q_{\geq 0}$ and the filter time constants τ^p_i , $\tau^q_i \in \mathbb{R}_{>0}$. The grid-forming IBR-based power system is stable whenever each controller gain satisfies,

$$\left(\max_{j\in\mathcal{N}_i} \{V_{0j}\} - V_{0i}\right)\beta_i^q \le \frac{1}{2m_i^q |B_{ii}|}, \forall i \in \mathcal{V}.$$
(18)

Remark 3. For any nodes j neighboring i where it holds that $\max_{j \in \mathcal{N}_i} \{V_{0j}\} > V_{0i}$, one can represent (18) as

$$m_i^q \beta_i^q \le K_i, \forall i \in \mathcal{V}$$
 (19)

where we define

$$K_i := \frac{1}{2 \left(\max_{j \in \mathcal{N}_i} \{ V_{0j} \} - V_{0i} \right) |B_{ii}|}.$$
 (20)

The term $m_i^q \beta_i^q$ represents the effective droop gain, as demonstrated in (5). Additionally, we can observe from (20) that the higher $|B_{ii}|$, the lower the value of K(i).

Proof. By treating our MIMO model as two SISO dynamical subsystems, the stability of the entire bus dynamics can be ensured by independently verifying the stability of each SISO system. After transforming our model from Fig. 1 to Fig. 3, we can consider the feedback loop as equivalent to Fig. 2 where G and $\frac{1}{s}$ L are given by (11). Suppose (18) is fulfilled, then **Lemma 1** implies that our network model $\frac{1}{s}$ L satisfies $0 \le L \le I$. Therefore, we can utilize **Theorem 1** to verify the stability.

Let g_i^V and g_i^θ describe the voltage magnitude and angle dynamics of bus i, respectively. We then can define

$$g_{\overline{i}}^{\underline{V}} = \frac{\gamma_i^q m_i^q \beta_i^q}{V_{0i} \tau_i^q}.$$

Since $g_i^V \ge 0$ for all i, then by **Theorem 1** we can easily choose any positive constant $f \in PR \cap \mathscr{A}_0$ such that $g^V \notin \mathcal{G}_f$. We also have

$$g_{\overline{i}}^{\underline{\theta}} \quad \frac{\gamma_i^p m_i^p \beta_i^p}{V_{0i}(\tau_i^p s + 1)}.$$

Let $f(s) = \frac{s}{s+T}$ for some $T \in \mathbb{R}_{>0}$. Let

$$F := \frac{s}{s+T} \left(1 + \frac{\gamma_i^p m_i^p \beta_i^p}{s V_{0i}(\tau_i^p s + 1)} \right) - \epsilon.$$

We will show that for all i, there exists an $\epsilon > 0$ such that

$$F \in PR \tag{21}$$

and, thus, $g_i^{\theta} \in \mathcal{G}_f$. Simplifying the expression of F, we get

$$F = \frac{\xi_{2,i}s^2 + \xi_{1,i}s + \xi_{0,1}}{\eta_{2,i}s^2 + \eta_{1,i}s + \eta_{0,1}},$$

where $\xi_{2,i} := (1 - \epsilon) \tau_i^q$, $\xi_{1,i} := 1 - \epsilon - T \epsilon \tau_i^q$, $\xi_{0,i} := \gamma_i^p m_i^p \beta_i^p - T \epsilon \tau_i^q$ $T \epsilon, \eta_{2,i} := V_{0i} \tau_i^q), \eta_{0i,i} := V_{00} (T + \text{We} \tau_i^q)$ choose T sufficiently large and ϵ small enough such that, for all

$$\left(\sqrt{\xi_{0,i}\eta_{2,i}} - \sqrt{\xi_{2,i}\eta_{0,i}}\right)^2 \le \xi_{2,i}\eta_{0,i} \le \xi_{1,i}\eta_{1,i},$$

from which the result (21) immediately follows [16, Cor. 11]. Therefore, satisfying (18) makes the feedback interconnection in Fig. 1 stable.

IV. NUMERICAL ILLUSTRATION

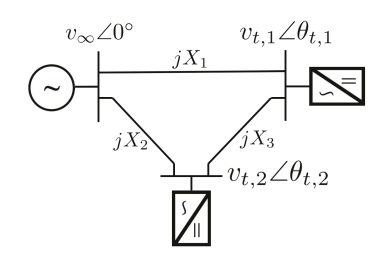


Figure 4. Three-bus power system.

Table I PARAMETER VALUES OF THE NETWORK

Parameter	Symbol	Value	Unit
Reactance	X_1, X_2, X_3	0.15, 0.20, 0.15	p.u.
Droop gain	$m_1^p, m_2^p, m_1^q, m_2^q$	0.05, 0.05, 0.05, 0.05	_
Filter gain	β_1^p, β_2^p	1, 1	_
Upper bound	$K_1/m_1^q, K_2/m_2^q$	0.75, 0.86	_
Time constant	$\tau_1^p,\tau_2^p,\tau_1^q,\tau_2^q$	50, 50, 50, 50	rad/s

We consider a three-bus system consisting of two GFM IBRs and an infinite bus in a network as shown in Fig. 4. Nominal parameter values of the system are given in Table I. We choose various operating points and DC gain β^q as listed in Table II, then use the small-disturbance (eigenvalue) analysis to analyze the stability around the equilibrium point under those values.

Table II SIMULATION CASES

-	Case	β_1^q, β_2^q	P_1^0, P_2^0	Q_1^0, Q_2^0	V_1^0, V_2^0
_	1	0.50, 0.50	1.0, 1.0	0.2, 0.2	1.0, 1.0
	2	0.75, 0.75	1.0, 1.0	0.2, 0.2	1.0, 1.0
_	3	0.75, 0.75	0.8, 0.8	0.1, 0.1	0.9, 0.9

Eigenvalues of the linearized system are presented in Table III. It is noteworthy that meeting condition (18) results in eigenvalues with negative real parts in all cases, for all the chosen operating points. This implies stable dynamics around the equilibrium points.

Table III Eigenvalues of the linearized system $(\times 10^4)$

Case 1	Case 2	Case 3
-1.7934 + j0.0000	-2.6878 + j0.0000	-2.6326 + j0.0000
-0.7321 + j0.0000	-1.0962 + j0.0000	-1.0648 + j0.0000
-0.0025 + j0.2063	-0.0025 + j0.2063	-0.0025 + j0.1823
-0.0025 - j0.2063	-0.0025 - j0.2063	-0.0025 - j0.1823
-0.0027 + j0.1282	-0.0027 + j0.1282	-0.0026 + j0.1173
-0.0027 - j0.1282	-0.0027 - j0.1282	-0.0026 - j0.1173

V. Conclusion

We present decentralized stability criteria for droopcontrolled grid-forming inverters. Our approach involves analyzing the Q-V coupling in the network Jacobian matrix and applying loop transformation for adjustments. The resulting criteria rely solely on properly tuning the droop gains of each local controller, as illustrated through numerical exam-ples. Future works include expanding our analysis on models with higher fidelity and incorporating heterogeneous grid-edge components, including grid-following IBRs.

REFERENCES

- [1] T. Ackermann, T. Prevost, V. Vittal, A. Roscoe, J. Matevosyan, and
 - N. Miller, "Paving the way: A future without inertia is closer than you think," *IEEE Power and Energy Magazine*, vol. 15, no. 6, pp. 61–79, 2017
- [2] F. Milano, F. Dörfler, G. Hug, D. J. Hill, and G. Verbič, "Foundations and challenges of low-inertia systems," in Power Systems Computation Conference (PSCC), 2018, pp. 1–25.
- "West murray zone sub-synchronous oscillations october 2022," Aus-
- [4] Bralsant Energy PM Valcety Operationa (chicall Charlicity. Abepal October 2022) in
- control of interconnected power systems," *IEEE Transactions on Circuits and systems*, vol. 27, no. 11, pp. 1102–1112, 1980.

 Y. Guo, D. Hill, and Y. Wang, "Global transient stability and voltage regulation for power systems," *IEEE Transactions on Power* Systems, vol. 16, no. 4, pp. 678-688, 2001.
- [6] U. Markovic, O. Stanojev, P. Aristidou, E. Vrettos, D. Callaway, and G. Hug, "Understanding small-signal stability of low-inertia systems," IEEE Transactions on Power Systems, vol. 36, pp. 3997–4017, 2021.
 [7] S. Geng and I. A. Hiskens, "Unified grid-forming/following inverter
- control," IEEE Open Access Journal of Power and Energy, vol. 9, pp. 489-500, 2022.
- [8] S. Jafarpour, V. Purba, B. Johnson, S. Dhople, and F. Bullo, "Singular perturbation and small-signal stability for inverter networks," IEEE Transactions on Control of Network Systems, vol. 9, no. 2, pp. 979-992, June 2022.
- [9] D. Pal, B. K. Panigrahi, B. Johnson, D. Venkatramanan, and S. Dhople, 'Large-signal stability analysis of three-phase grid-following inverters,'
- IEEE Transactions on Energy Conversion, pp. 1–15, 2023.
 [10] Z. Wang, S. Mei, F. Liu, S. H. Low, and P. Yang, "Distributed load side control: Coping with variation of renewable generations," Automatica,
- vol. 109, pp. 1-14, 2019. [11] H.-D. Chang, C.-C. Chu, and G. Cauley, "Direct stability analysis of electric power systems using energy functions: theory, applications, and perspective," Proceedings of the IEEE, vol. 83, no. 11, pp. 1497–1529,
- [12] R. Pates and E. Mallada, "Robust scale-free synthesis for frequency control in power systems," *IEEE Transactions on Control of Network* Systems, vol. 6, no. 3, pp. 1174–1184, 2019.
 [13] P. Kundur, Power System Stability and Control, 2nd edition. New York,
- USA: McGraw-Hill, 2022.
- [14] S. Kundu, S. Geng, S. P. Nandanoori, I. A. Hiskens, and K. Kalsi, "Distributed barrier certificates for safe operation of inverter-based microgrids," in 2019 American Control Conference (ACC). IEEE, 2019, pp. 1042-1047.
- [15] R. A. Horn and C. R. Johnson, Topics in matrix analysis, 1991. Cambridge, UK: Cambridge University Presss, 1991.
- [16] M. Chen and M. Smith, "A note on tests for positive-real functions." IEEE Transactions on Automatic Control, vol. 54, pp. 390-393, 2009.